Unravelling the atomic structure of cross-linked (1 × 2) TiO$_2$(110)

Hans Hermann Pieper,[a] **Krithika Venkataramani,**[ab] **Stefan Torbrügge,†**[a]
Stephan Bahr,†[a] **Jeppe V. Lauritsen,**[b] **Flemming Besenbacher,**[b] **Angelika Kühnle**[c]
and Michael Reichling[a]

The cross-linked (1 × 2) reconstruction of TiO$_2$(110) is a frequently observed phase reflecting the surface structure of titania in a significantly reduced state. Here we resolve the atomic scale structure of the cross-linked (1 × 2) phase with dynamic scanning force microscopy operated in the non-contact mode (NC-AFM). From an analysis of the atomic-scale contrast patterns of the titanium and oxygen sub-structures obtained by imaging the surface with AFM tips having different tip apex termination, we infer the hitherto most accurate model of the atomic structure of the cross-linked (1 × 2) phase. Our findings suggest that the reconstruction is based on added rows in [001] direction built up of Ti$_3$O$_6$ units with an uninterrupted central string of oxygen atoms accompanied by a regular sequence of cross-links consisting of linear triples of additional oxygen atoms in between the rows. The new insight obtained from NC-AFM solves previous controversy about the cross-linked TiO$_2$(110) surface structure, since previously proposed models based on cross-links with a lower O content do not appear to be consistent with the atom-resolved data presented here. Instead, our measurements strongly support the Ti$_3$O$_6$ motif to be the structural base of the cross-linked (1 × 2) reconstruction of TiO$_2$(110).

Introduction

The TiO$_2$(110) surface is one of the most extensively studied oxide surfaces and it serves as an excellent surface science model for structure formation, reconstruction and surface chemistry of the important group of reducible metal oxides.[1,2]

The TiO$_2$(110) surface structure, stoichiometry and reactivity strongly depend on the oxidation state of the bulk.[3] The overall reduction resulting from preparation at elevated temperature under conditions of the ultra-high vacuum (UHV) is quantified by the so-called *sample history* that is the product of annealing temperature and annealing time accumulated for a specific crystal.[4,5] Progressive thermal treatment in UHV results in structural modifications at the surface and a reduction of the bulk crystal[6] that becomes manifest in a large number of Ti^{3+} (3d) interstitials in the near surface region.[7] When heating the crystal in an oxygen atmosphere, the stoichiometry can at least partially be re-established.[8]

The cross-linked (1 × 2) reconstructed surface is produced by subjecting the crystal to a number of sputter/anneal cycles in UHV yielding a crystal with typically 0.1% bulk oxygen deficiency.[9] Notably, the surface can not only be produced under reducing conditions but for an already reduced crystal also under oxidising conditions and it has, therefore, been speculated that the (1 × 2) reconstruction and the formation of cross-links are kinetically favoured.[10] Under oxidising conditions, the surface can be grown in layers in a cycle involving the (1 × 1) terminated surface, the plain (1 × 2) reconstructed surface and the cross-linked (1 × 2) surface.[3,5] Exposing a regular track structure with 1.3 nm gauge, the cross-link reconstruction has been used as a template for the growth of nano objects like formic acid,[11] copper phthalocyanine,[12] C$_{60}$ molecules,[13] and metal particles,[14,15] on titania where often an initial nucleation at the cross-links is observed. In water exposure experiments, a preferential adsorption of water at the cross-links has been reported.[16]

The atomic structures on TiO$_2$(110) have been investigated in the past with a number of different techniques and also theoretically and the genesis and discussion of ideas on surface morphology and atomic structural details have extensively been reviewed elsewhere.[2,3] However, two different added row models are still under discussion for the atomic structure of the cross-linked (1 × 2) reconstruction, namely a model with rows composed of Ti$_2$O$_3$ units that are interrupted at the locations of the cross-links[13,17] and a model with rows composed of Ti$_3$O$_6$ units and an uninterrupted central string of oxygen atoms where cross-links are formed by additional oxygen atoms and a reduced number of titanium atoms in between the rows.[10] The structural details of these two models are displayed in Fig. 1 where plane and cross-sectional views are depicted. The formal stoichiometry of the structure composed of Ti$_2$O$_3$ units and cross-links added to the unreconstructed surface is Ti$_2$O$_3$ assuming a 12 × 2 reconstruction (see discussion below) and neglecting any titanium interstitials that may be present; this represents a reduced surface state. The formal stoichiometry for the structure composed of Ti$_3$O$_6$ units is Ti$_{36}$O$_{75}$ representing a slightly oxygen rich state relative to TiO$_2$. Although, the reconstruction has been studied in detail with scanning tunnelling microscopy (STM) and

[a] *Fachbereich Physik, Universität Osnabrück, Barbarastr. 7,
49076 Osnabrück, Germany. E-mail: reichling@uos.de*
[b] *Interdisciplinary Nanoscience Center (iNANO) and Department of
Physics and Astronomy, Aarhus University,
8000 Aarhus C, Denmark*
[c] *Institut für Physikalische Chemie, Johannes Gutenberg-Universität
Mainz, Jakob-Welder-Weg 11, 55099 Mainz, Germany*
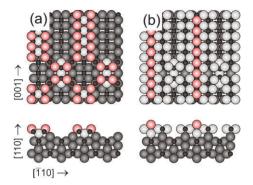† Present address: SPECS GmbH, Voltastr. 5, 13355 Berlin, Germany.

Fig. 1 (colour online) Added row models for the cross-linked (1×2) reconstructed $TiO_2(110)$ surface based on Ti_2O_3 (a) and Ti_3O_6 (b) units. Small circles denote titanium atoms, while large circles denote oxygen atoms. The different degree of shading symbolises the association of an atom to a specific surface layer.

surface diffraction techniques,[3] its atomic details have never unambiguously been unravelled.

Here, we investigate the cross-linked structure with dynamic scanning force microscopy operated in the non-contact mode (NC-AFM) and resolve the ambiguities with respect to the two models depicted in Fig. 1 that have been derived from STM investigations. The main benefit of using NC-AFM in this study is that the NC-AFM contrast can reveal complementary atomic details from both the O and Ti sub-lattices when imaging with tips of different atomic tip apex termination as we have recently demonstrated in a series of studies on atomic contrast formation on the (1×1) terminated $TiO_2(110)$ surface.[18–21] There we also found that for certain tip conditions, it is even possible to image both sub-lattices at the same time. This provides a much more straightforward and reliable framework for image interpretation as compared to previous STM studies. The atomic resolution STM contrast on titania is usually studied by empty state imaging highlighting the titanium sub-lattice only where the contribution to the tunnelling current at positive sample bias is primarily attributed to the Ti species while the oxygen sub-lattice is most difficult to be explored.[22–24] Imaging different sub-lattices with tips of different atomic apex termination is a well established concept in NC-AFM and not restricted to oxide surfaces. The distinction[25] and identification[26,27] of the sub-lattices by proper theoretical modelling has, for instance, fully been developed in the framework of atom resolved imaging on fluorides. Here we exploit the extended knowledge of NC-AFM atomic image contrast formation on the $TiO_2(110)$ surface[18–21] to facilitate the interpretation of NC-AFM images obtained on the cross-linked (1×2) reconstructed surface and identify the atomic sub-structures of the added rows. Such a detailed analysis is fully compatible with a composition of the added rows of Ti_3O_6 units and oxygen rich cross-links but not with other models and we adopt the Ti_3O_6 model as the valid model for the cross-link reconstruction of the $TiO_2(110)$ (1×2) structure.

Experimental

Experiments are performed under UHV conditions in a vacuum chamber maintaining a base pressure lower than 3×10^{-10} mbar. For the preparation of the cross-linked

(1×2) reconstruction, the as-grown TiO_2 single crystal (MTI Corp., Richmond, CA, USA) is *ex situ* polished and then sputtered with Ar^+ ions (2×10^{-5} mbar argon pressure, 1 keV ion energy, 15 min sputter time) and afterwards annealed at 1100 K for 15 min in UHV to obtain a clean, well ordered surface. After 13 of such preparation cycles, we obtain a degree of bulk reduction of the crystal (identified by its dark blue colour) stabilising a large fraction of the surface in the cross-linked (1×2) reconstruction.

The NC-AFM measurements are performed after cooling the sample to a temperature close to room temperature with an upgraded[28] commercial STM/AFM system (Omicron Nano Technology GmbH, Taunusstein, Germany) operated in the non-contact frequency modulation mode.[29] The cantilever is excited to oscillate at its resonance frequency with a constant amplitude of typically 10 nm. The detuning of the cantilever resonance frequency is measured by a PLL detector (Nanosurf AG, Liestal, Switzerland). All images shown except Fig. 5 represent contours of constant detuning as the detuning is kept constant by a regulation loop acting on the piezo controlling the tip–surface distance (topography mode). Fig. 5 is obtained in a quasi constant-height scanning mode where the loop gain is reduced so that the tip follows the overall topography of the sample while the atomic scale information appears in the detuning signal.[30] It has to be kept in mind, however, that images obtained at the atomic scale often do not represent atomic topography but are rather determined by details in the interaction between atoms of the nanocluster at the tip end and surface atoms. Force sensors are commercial silicon cantilevers (PPP-NCH, NanoWorld AG, Neuchâtel, Switzerland) having a resonance frequency of typically 300 kHz and a Q-factor of typically 30 000. Tips are sputtered with Ar^+ ions (5×10^{-5} mbar argon pressure, 0.5 keV ion energy, 3 min sputter time) in UHV prior to measurements to remove contaminants and the oxide layer. After transfer to the UHV, the nanotip creating atomic contrast is formed by a slight contact of the tip with the sample surface. A specific atomic termination cannot deliberately be created in this way, however, frequent tip changes occurring accidentally or by provoking them regularly produce tip terminations yielding a stable atomic contrast. Tip terminations with descriptive titles *positive* ($+$), *negative* ($-$) or *sharp negative* (s) reflecting the apparent atomic contrast are denoted by respective triangular symbols placed in the upper right corner of the NC-AFM images. The scanner is calibrated in the *x*–*y* plane by measurements on patches of unreconstructed $TiO_2(110)$ revealing atomic rows with the well-known distance of 0.65 nm.

Results

Surface morphology

Fig. 2 displays two NC-AFM images of the as-prepared surface at different magnification and represents the typical morphology for the chosen point in the sample history. Fig. 2(a) exhibits overall well-ordered atomically flat terraces with a width of typically 100 nm. The atomic scale structure is dominated by rows in [001] direction having a distance of 1.3 nm, some of them giving the impression of growing from
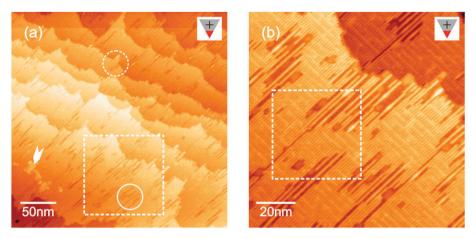
This journal is © the Owner Societies 2010

Phys. Chem. Chem. Phys., 2010, **12**, 12436–12441 | 12437

Fig. 2 (colour online) NC-AFM overview images with different magnification revealing the morphology of the as-prepared $TiO_2(110)$ surface that is dominated by the cross-linked (1×2) reconstruction with openings revealing small patches of unreconstructed surface underneath (dark areas in frame (b)). The white arrow points to a region of growth on top of a terrace with cross-linked (1×2) reconstruction. White solid and dashed circles mark regions of incomplete growth of a terrace exhibiting isolated rows and the growth of a row from an upper terrace onto the neighbouring lower one, respectively. Squares marked by dashed lines are areas of magnified scans shown in Fig. 2(b) and 3(a), respectively.

one terrace onto the neighbouring lower terrace (see region in dashed white circle). We anticipate, however, that the area underneath such far protruding rows is (1×1) reconstructed. This is a well known feature pointing to the fact that the surface morphology is determined by the growth of structures having different reconstruction during the high temperature preparation rather than just by slight local atomic rearrangements.[3] Further indications of growth processes are found in the form of small row clusters present on top of terraces (see white arrow). While most of the surface is covered with rows connected by cross-links, there are also less well ordered regions exhibiting isolated rows (see region in solid white circle). Fig. 2(b) reveals details of the cross-linked structure. Generally, cross-links appear in a regular fashion effectively yielding an $n \times 2$ network.[3] The periodicity n is typically 12, however, there are also significant deviations in n and there are areas where cross-links are missing. Frame (b), furthermore, reveals the coexistence of the cross-linked (1×2) structure with single or few rows possibly of plain (1×2) structure and small patches of the (1×1) structure in a layered fashion that is testament of the cyclic growth of structures having different reconstructions on top of each other.[5]

Atomic scale contrast

In the images compiled in Fig. 3, we compare atomic scale contrast formation obtained for different tip terminations. Fig. 3(a) is a magnified section of Fig. 2(b) exhibiting small patches of unreconstructed surface underneath the (1×2) layer (see areas exhibiting fine lines). From this image, the effective tip termination can be inferred by a careful analysis of the (1×1) patches. There, we find bright atomic rows interrupted by dark defects (see also upper right part of Fig. 4(a)) which can be explained by a positive tip termination imaging oxygen rows as bright.[18] For a detailed analysis of atomic scale contrast formation on the added rows, we compare this contrast to the contrast obtained in the same area with two other tips. Respective results are shown in

images of Fig. 3(b) and (c) that we associate with a negatively terminated and a sharp negatively terminated tip, respectively.

In the image recorded with the positively terminated tip apex (Fig. 3(a)), we observe bright added rows and slightly brighter cross-links. A particularly good resolution of the subjacent unreconstructed surface reveals that the added rows of the reconstruction are centred on dark rows that are strings of titanium atoms of the unreconstructed surface. We assign the bright added row contrast to oxygen atoms and hypothesise that the cross-links appear slightly brighter than the rows due to a high concentration of oxygen atoms in the cross-link region. Note, that the added rows appear uninterrupted and the bright contrast of the cross-links appears in between the added rows.

In the NC-AFM image recorded with the tip associated with negative apex termination (Fig. 3(b)), we observe similarly bright rows as in frame (a). However, there is a distinct dark contrast feature at the position of the cross links, again with its centre in between the bright rows. Note, that in this case, the bright rows are interrupted by the cross-link features, the dark rows, however, appear without any interruption but are broadened at the position of the cross-links. For this tip apex termination, we assign the bright contrast to titanium atoms. Interestingly, the bright strings from the titanium atoms of the added rows melt together in cross-linked (1×2) areas while they appear separately for non-cross-linked rows. This is evident from analysing areas taken form the upper right part of Fig. 3(a) and (b) that are reproduced with higher magnification in Fig. 4(a) and (b), respectively. There is a non-cross-linked added row (see arrow in frame (a)) appearing as a broad feature for positive tip termination but as two distinct bright lines (see arrows in frame (b)) having a distance of (0.65 ± 0.02) nm for negative tip termination. These bright lines are associated with titanium strings and develop into two neighbouring bright rows when imaging with negative tip termination in a cross-linked area.

The bright contrast of the titanium strings is strongly enhanced when imaging with a tip that we associate with a
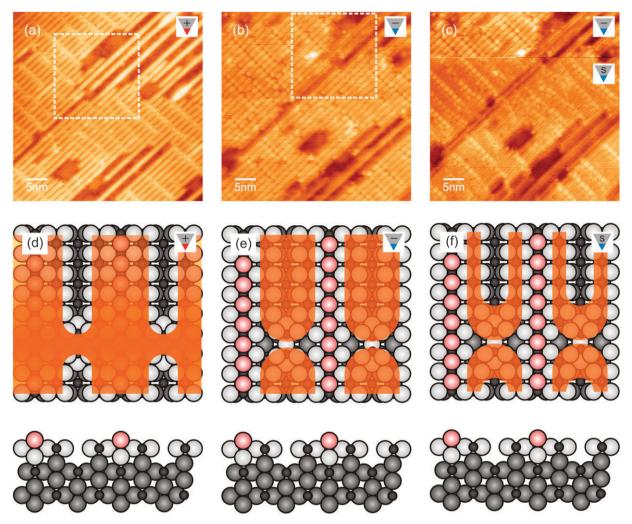
Fig. 3 (colour online) Magnified NC-AFM images of the area marked in Fig. 2(b) by a dashed square taken with three different tips, namely a positively terminated tip apex (a), a negatively terminated tip apex (b) and a sharp negatively terminated tip apex (c). A tip change results in the distinct change in atomic scale contrast observed in the upper third of frame (c). The dashed squares in frames (a) and (b) mark the area shown in Fig. 4 with higher magnification. Frames (d), (e) and (f) are schematic representations for atomic scale contrast formation on added rows and at cross-links for the different tip conditions as explained in the main text. Orange shaded areas denote bright contrast features observed in the NC-AFM images.
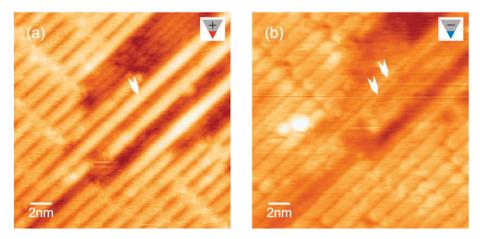

Fig. 4 (colour online) Details extracted from Fig. 3(a) and (b) showing the same surface area scanned with tips of different apex termination. White arrows point to different contrast formation for positive (a) and negative (b) tip apex terminations. The bright contrast feature representing the most protruding oxygen row of the reconstruction (a) is split into two features representing the neighbouring titanium rows (b).

sharp negatively terminated tip apex (lower part of Fig. 3(c)). In this contrast mode, the titanium strings appear with a strong contrast as very fine lines and these lines can be resolved even in the cross-linked regions.

Atomic structure model for the added rows

The consistent picture of contrast formation for the three different tips is summarised in the schemes depicted in Fig. 3(d)–(f) corresponding to the experimental results from frames (a)–(c). Features of bright contrast are indicated by orange shading superimposed to the structural model of added rows based on Ti_3O_6 units that we adopt as the valid model for reasons to be outlined below. A tip with positive termination images the oxygen atoms of the added rows as uninterrupted bright rows with even brighter lobes at the locations of the cross-links. The fact that the row feature is uninterrupted and cross-links appear as oxygen rich is a first piece of evidence which shows that the Ti_3O_6 and not the Ti_2O_3 model is valid as the latter clearly predicts an interruption at the location of the cross-links and these are not oxygen rich (see Fig. 1(a)).

We succeeded in imaging the added row structure in greater detail by approaching the positively terminated tip closer to the surface; a respective image is displayed in Fig. 5. This image exhibits atomic resolution along a centre oxygen string of the added row confirming atom-by-atom that there is no interruption at the locations of cross-links. The fact that there appears a centre row with a distinctly enhanced contrast is the second piece of evidence for the validity of the Ti_3O_6 model.[9] Such a feature would not be expected for the Ti_2O_3 model predicting a double oxygen string terminating the added row (see Fig. 1(a)) but instead perfectly fits the Ti_3O_6 model predicting a central string of oxygen atoms protruding further out of the surface than any other of the atoms (see Fig. 1(b)).

An AFM tip with negative apex termination images the titanium atoms as bright and the oxygen atoms as dark (see Fig. 3(b) and (e)). Consequently, the centre oxygen strings of the added rows and 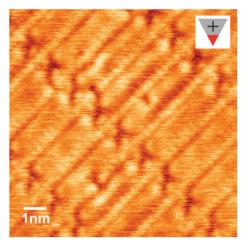their cross-link lobes appear as a dark uninterrupted grid for this imaging mode while the bright contrast in between stems from titanium atoms. In situations where the titanium atoms can be discerned as individual strings of bright contrast (see lower part of Fig. 3(c) and (f)), these strings are equally spaced with (0.65 ± 0.02) nm distance which is in perfect agreement with the Ti_3O_6 model predicting a spacing of 0.65 nm but disagrees with the Ti_2O_3 model predicting a spacing of 0.35 nm. This is the third piece of evidence for the validity of the Ti_3O_6 atomic structure model for the added rows of the cross-linked (1×2) reconstruction.

Conclusion

The cross-linked (1×2) reconstruction is the dominant reconstruction of $TiO_2(110)$ prepared in UHV under reducing conditions for a titania sample that is strongly reduced in the bulk. However, it is not the only phase present at the surface but found in layered structures coexisting with the plain (1×2) reconstruction and the (1×1) structure. Atomic scale NC-AFM imaging of the surface allows an identification of oxygen and titanium sub-structures in the added rows formed by the (1×2) reconstruction and the cross-links when exploiting different imaging modes determined by the type of atomic termination of the tip apex. A characteristic feature of the oxygen sub-structure is an uninterrupted string of atoms at the centre of the added row and lobes at the positions of the cross-links. The titanium sub-structure appears in the form of rows consisting of two strings of titanium atoms with a distance of 0.65 nm; these rows are interrupted at the locations of the cross-links. This experimental evidence is fully consistent with a model proposing that the added rows are built up from Ti_3O_6 units and oxygen rich cross-links but is not consistent with other atomic structure models proposed. This model is, therefore, considered to be the valid model describing the cross-linked (1×2) reconstruction of $TiO_2(110)$.

It is surprising to find an oxygen rich structure as the preferred reconstruction on a crystal that is reduced in the bulk. However, it has to be kept in mind that the actual level of bulk reduction is small and maintained by a surplus of Ti^{3+} interstitials rather than oxygen deficiency. The tendency of Ti^{3+} interstitials to accumulate in the bulk rather than at the surface together with the strong chemical potential of oxygen in the gas phase yields a thermodynamic tendency towards surface oxidation. Together with favourable kinetic effects, this may explain the discrepancy between bulk and surface oxidation states and the preferred formation of an oxygen rich cross-link structure.

Fig. 5 (colour online) High resolution NC-AFM image taken in an area of cross-linked (1×2) reconstruction with a positively terminated tip. The main bright feature is an uninterrupted, atomically resolved central string of oxygen atoms in the centre of the added rows accompanied by bright lobes at the positions of the cross-links.

12440 | *Phys. Chem. Chem. Phys.*, 2010, **12**, 12436–12441

This journal is © the Owner Societies 2010

Notes and references

1 V. E. Henrich and P. A. Cox, *The surface science of metal oxides*, Cambridge University Press, Cambridge, 1996.
2 U. Diebold, *Surf. Sci. Rep.*, 2003, **48**, 53.
3 M. Bowker, *Curr. Opin. Solid State Mater. Sci.*, 2006, **10**, 153.
4 S. Wendt, R. Schaub, J. Matthiesen, E. K. Vestergaard, E. Wahlstroem, M. D. Rasmussen, P. Thostrup, L. M. Molina, E. Laegsgaard, I. Stensgaard, B. Hammer and F. Besenbacher, *Surf. Sci.*, 2005, **598**, 226.
5 M. Bowker and R. A. Bennett, *J. Phys.: Condens. Matter*, 2009, **21**, 474224.
6 M. Li, W. Hebenstreit, U. Diebold, A. M. Tyryshkin, M. K. Bowman, G. G. Dunham and M. A. Henderson, *J. Phys. Chem. B*, 2000, **104**, 4944.
7 S. Wendt, P. T. Sprunger, E. Lira, G. K. H. Madsen, Z. S. Li, J. O. Hansen, J. Matthiesen, A. Blekinge-Rasmussen, E. Laegsgaard, B. Hammer and F. Besenbacher, *Science*, 2008, **320**, 1755.
8 M. Li, W. Hebenstreit, L. Gross, U. Diebold, M. A. Henderson, D. R. Jennison, P. A. Schultz and M. P. Sears, *Surf. Sci.*, 1999, **437**, 173.
9 R. A. Bennett, S. Poulston, P. Stone and M. Bowker, *Phys. Rev. B: Condens. Matter Mater. Phys.*, 1999, **59**, 10341.
10 R. A. Bennett, P. Stone, N. J. Price and M. Bowker, *Phys. Rev. Lett.*, 1999, **82**, 3831.
11 R. A. Bennett, P. Stone, R. D. Smith and M. Bowker, *Surf. Sci.*, 2000, **454**, 390.
12 Y. F. Wang, Y. C. Ye and K. Wu, *J. Phys. Chem. B*, 2006, **110**, 17960.
13 K. Fukui and M. Sakai, *J. Phys. Chem. B*, 2006, **110**, 21118.
14 R. A. Bennett, M. A. Newton, R. D. Smith, J. Evans and M. Bowker, *Mater. Sci. Technol.*, 2002, **18**, 710.
15 Y. Maeda, T. Fujitani, S. Tsubota and M. Haruta, *Surf. Sci.*, 2004, **562**, 1.
16 P. Maksymovych, S. Mezhenny and J. T. Yates, *Chem. Phys. Lett.*, 2003, **382**, 270.
17 S. Takakusagi, K.-i. Fukui, F. Nariyuki and Y. Iwasawa, *Surf. Sci.*, 2003, **523**, L41.
18 J. V. Lauritsen, A. S. Foster, G. H. Olesen, M. C. Christensen, A. Kühnle, S. Helveg, J. R. Rostrup-Nielsen, B. S. Clausen, M. Reichling and F. Besenbacher, *Nanotechnology*, 2006, **17**, 3436.
19 G. H. Enevoldsen, A. S. Foster, M. C. Christensen, J. V. Lauritsen and F. Besenbacher, *Phys. Rev. B: Condens. Matter Mater. Phys.*, 2007, **76**, 205415.
20 G. H. Enevoldsen, H. P. Pinto, A. S. Foster, M. C. R. Jensen, A. Kühnle, M. Reichling, W. A. Hofer, J. V. Lauritsen and F. Besenbacher, *Phys. Rev. B: Condens. Matter Mater. Phys.*, 2008, **78**, 045416.
21 R. Bechstein, C. González, J. Schütte, P. Jelínek, R. Pérez and A. Kühnle, *Nanotechnology*, 2009, **20**, 505703.
22 U. Diebold, J. F. Anderson, K.-O. Ng and D. Vanderbilt, *Phys. Rev. Lett.*, 1996, **77**, 1322.
23 H. Onishi and Y. Iwasawa, *Phys. Rev. Lett.*, 1996, **76**, 791.
24 O. Gülseren, R. James and D. W. Bullett, *Surf. Sci.*, 1997, **377–379**, 150.
25 S. Hirth, F. Ostendorf and M. Reichling, *Nanotechnology*, 2006, **17**, S148.
26 A. S. Foster, C. Barth, A. L. Shluger and M. Reichling, *Phys. Rev. Lett.*, 2001, **86**, 2373.
27 C. Barth, A. S. Foster, M. Reichling and A. L. Shluger, *J. Phys.: Condens. Matter*, 2001, **13**, 2061.
28 S. Torbrügge, J. Lübbe, L. Tröger, M. Cranney, T. Eguchi, Y. Hasegawa and M. Reichling, *Rev. Sci. Instrum.*, 2008, **79**, 083701.
29 T. R. Albrecht, P. Grütter, D. Horne and D. Rugar, *J. Appl. Phys.*, 1991, **69**, 668.
30 S. Gritschneder, Y. Namai, Y. Iwasawa and M. Reichling, *Nanotechnology*, 2005, **16**, S41.

This journal is © the Owner Societies 2010

Phys. Chem. Chem. Phys., 2010, **12**, 12436–12441 | 12441